Silicon (2024) 16:4703–4711
https://doi.org/10.1007/s12633-024-03028-2

RESEARCH

Effect of Silicon Nitride Coated Carbon Crucible on Multi-Crystalline Silicon Ingot during Directional Solidification Process: Numerical Simulation

P. Periyannan[1] · M. Bharathwaj[1] · P. Karuppasamy[1] · P. Ramasamy[1]

Received: 16 March 2024 / Accepted: 19 May 2024 / Published online: 31 May 2024

Abstract

Numerical simulation has been carried out on the directional solidification (DS) for the growth of multi-crystalline silicon (mc-Si) ingot through a 2-dimensional axis-symmetric global transient model. In this work, we used a silicon nitride-coated carbon crucible DS system. Due to this, the thermal conductivity and density of the crucible are changed which may affect the furnace's thermal field. Changes in the thermal field can impact the temperature distribution, von Mises stress, maximum shear stress, normal stresses, average growth rate, and power consumption. Using numerical simulation based on the finite volume method the solidification process is analyzed and investigated with a silicon nitride-coated carbon crucible (modified system) and silicon nitride-coated quartz crucible (conventional system). Solar cell performance depends directly on the quality of the mc-Si ingot. The modified grown ingot is more favorable for PV applications.

Keywords Directional solidification process · Carbon crucible · Quartz crucible · Silicon nitride coating · Von Mises stress

1 Introduction

Solar energy is inexpensive and elegant for the future world. The advantages of this energy are easy handiness, manageability, and technology for the rapidly growing world that demands energy and electricity. Solar energy is being suggested to the world to clear up the issue of decarbonization policies and global warming. Currently, solar cells utilizing numerous materials, for instance, perovskites are being vigorously researched; but in usage, crystalline silicon solar cells are dominating. Silicon is an important material for photovoltaic industries due to its sufficiency and low cost. Two types of crystalline silicon are mono-silicon and mc-Si. Monocrystalline silicon is high quality and manufactured by the Czochralski (CZ) method, but the production cost is high. Most industries go for multi-crystalline silicon manufactured by the directional solidification (DS) method, here the production cost is low [1]. Sustainable research on the DS process could enhance multi-crystalline silicon ingot quality.

The ingot pureness and the wafer quality are influenced by the admixed in the feedstock materials and inhomogeneous temperature difference during the solidification process. At the time of the solidification process, numerous parameters are normally modified to get an appropriate temperature field. These parameters are decided by vacuum, argon gas flow, water circulation, etc. [2]. The heat transport process plays a crucial role in the directional solidification method. The von mises stress and maximum shear stress are mainly governed by the temperature distribution of the furnace [3]. To get better quality ingot there should be less impurities and less dislocation. These defects such as dislocation and impurities affect the conversion efficiency of the solar cell. Appropriate thermal stress can control these defects during the growth of mc-Si by the DS process [4]. However, temperature distribution and thermal field have a crucial effect on the quality of the mc-Si ingot during the DS process. The summation of various insulation blocks in the DS furnace may increase the chances for a slightly higher temperature gradient, growth rate, and thermal stress in the mc-Si ingot [5, 6]. These should be avoided to get better quality ingot. Numerical simulation helps to investigate heat transmission and fluid flow in the DS process. H. Zhang et al. investigated

✉ P. Karuppasamy
karuppasamyp@ssn.edu.in

1 Department of Physics, SSN Research Centre, Sri Sivasubramaniya Nadar College of Engineering, Kalavakam 603110, Tamil Nadu, India

the relationship between the growth rate and temperature at a heat exchanger block to establish a large-scale DS system and compared it with experimental results [7].

Liu et al. have initiated fixed and movable partition blocks that can affect the axial temperature gradient. The result reveals that the movable partition block can crucially minimize the thermal stress when compared with the fixed one [6]. Huang et al. demonstrated that an increase in the velocity of the partition block significantly affects the stress distribution in the mc-Si growth process and puts back less thermal conductivity susceptor materials to study the temperature distribution of the DS method and they have described that less thermal conductivity susceptor material effortlessly protects the seeds [8, 9]. The appropriate thermal field is required for the DS growth process. Inside the furnace heater and insulation wall are components to control the thermal field distribution for the DS process. The outline of the thermal field in a furnace participates in the growth process and structural optimization. Numerous researchers optimized the structure of the heater and insulation block to get an appropriate thermal field for the DS process [5, 10–12]. J. Wei et al. analyzed the heater power by changing the position of the side insulation. The results show that the power consumption is significantly affected by the kinetic motion of the side insulation [13]. Nguyena et al. studied the new optimized furnace addition of insulation block fixed at side insulation in the DS furnace to enhance the heat transfer of the DS furnace that may control the heat loss, power consumption, and thermal stress [14]. To get high-quality ingot and high efficiency of solar cells it is required to have a suitable thermal field in silicon melt during the solidification process.

In this work, we have simulated and analyzed the silicon nitride-coated carbon crucible (modified system) and compared it with the silicon nitride-coated quartz crucible (conventional system). When using carbon crucibles, the system consumes less power and increases the average growth rate which is suitable for silicon growth at the industrial level. Due to less temperature gradient, the thermal stresses of the mc-Si ingot are also reduced which is favourable for getting the better-quality ingot.

2 Model Description

The DS furnace consists of a retort for crucible support, graphite heater, insulation block, and heat exchanger block. The conventional system consists of a quartz crucible and the modified system consists of a carbon crucible, as shown in Fig. 1. The feedstock of silicon is fed into the crucible then the crucible is placed inside the furnace and heated up to 1500 °C to melt silicon feedstock. The major assumptions for numerical simulation are (1) the configuration of furnace geometry is axis-symmetric, (2) the transfer of radiation is represented as diffuse-gray surface radiation, and (3) melt flow is incompressible and laminar. The simulation growth is conducted by the finite volume method. Square and rectangle-shaped grids are generated for the simulation process. We can obtain better geometrical boundaries with the help of structured mesh. For argon gas flow unstructured mesh is used due to its non-geometric shape. Table 1 reveals the thermal properties of quartz crucible, carbon crucible, and silicon nitride. The silicon nitride properties are assigned at the inner surface for both crucibles and the other materials properties are given in the previously published work [15].

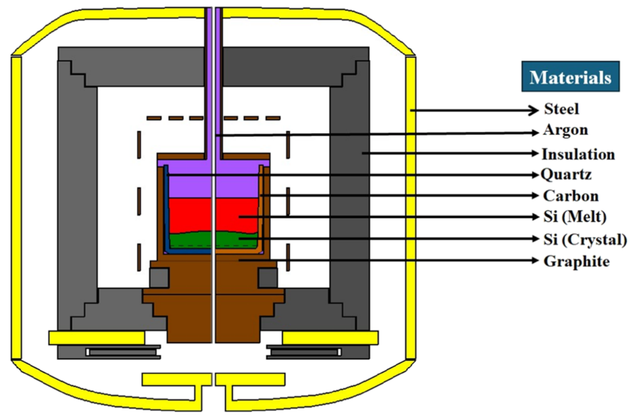

Fig. 1 Schematic Diagram of DS furnace (left-conventional system) (right-modified system)

3 Numerical Simulation

The governing equations of mass transport, heat transport, and species transport are as follows [16]:

$$\frac{\partial \rho}{\partial t} + \nabla \bullet (\rho \vec{u}) = 0 \tag{1}$$

$$\frac{\partial (\rho \vec{u})}{\partial t} + (\vec{u} \bullet \nabla)\rho \vec{u} = -\nabla \bullet p + \nabla \bullet \tau + (\rho - \rho_0)\vec{g} \tag{2}$$

$$\frac{\partial (\rho c_p T)}{\partial t} + \nabla \bullet (\rho c_p \vec{u} T) = \nabla \bullet (\lambda_{\text{eff}} \nabla T) - \nabla \bullet \overrightarrow{q_{rad}} + S_T \tag{3}$$

$$\frac{\partial (\rho \varphi_i)}{\partial t} + \nabla \bullet (\rho \vec{u} \varphi_i) = \nabla \bullet (D_{\varphi_i \text{eff}} \nabla \varphi_i) + S_{\varphi_i} \tag{4}$$

C_p → specific heat capacity, $\vec{u}$ → velocity, ρ → density, T → temperature $\lambda_{\text{eff}} = \lambda + \frac{C_p \mu_t}{Pr_t}$ is the effective thermal conductivity $\vec{q}_{rad}(r) = \int_0^\infty \oint_{4\pi} \Omega I_\lambda(r,\Omega) d\Omega d\lambda$ is the vector radiative heat flux [16]. $I_\lambda(r,\Omega)$ → the intensity of radiation at point r, λ →

Table 1 Thermal properties of quartz crucible and carbon crucible

Properties	Quartz crucible	Carbon crucible	Silicon nitride
Thermal Conductivity (W/mK)	4	146.885–0.17687 T	10
Emissivity	0.85	0.8	0.6
Density (Kg/m^3)	2650	1950	3184
Heat capacity (J/KgK)	1232	710	673

wavelength of the radiation $D_{\varphi_i \mathrm{eff}}$ → effective dynamic diffusivity $S_{\varphi_i} = S^u_{\varphi_i} + \phi_i S^P_{\varphi_i}$ → stands for the i$^{\text{th}}$ species source.

The following equation gives the growth velocity at the solid–liquid interface [17].

$$V_{\mathrm{crys}} = \frac{1}{n_x \rho_{\mathrm{crys}} \Delta H}\left(\lambda_{\mathrm{crys}}\frac{\partial T_{\mathrm{crys}}}{\partial n} - \lambda_{\mathrm{melt}}\frac{\partial T_{\mathrm{melt}}}{\partial n} + \left(Q^{\mathrm{in}}_{rad} - Q^{\mathrm{out}}_{rad}\right)_{\mathrm{crys}} - \left(Q^{\mathrm{in}}_{rad} - Q^{\mathrm{out}}_{rad}\right)_{\mathrm{melt}}\right) \tag{5}$$

Thermal stress reflects the von Mises stress of the ingot [8, 18]. The thermal stress is analyzed using a displacement-based thermo-elastic stress model. The governing partial differential equations for momentum balance in an axis-symmetric model [19] can be written as,

$$\frac{1}{r}\frac{\partial}{\partial r}\left(r\sigma_{rr}\right) + \frac{\partial}{\partial z}\left(\sigma_{rz}\right) - \frac{\sigma_{\phi\phi}}{r} = 0 \tag{6}$$

$$\frac{\partial}{\partial r}\left(r\sigma_{rz}\right) + \frac{\partial}{\partial z}\left(\sigma_{zz}\right) = 0 \tag{7}$$

To get von Mises stress the above equation is integrated and substituted in the stress–strain equation [19].

$$\sigma_{von} = \frac{3}{2}\left(S_{ij}S_{ij}\right)^{\frac{1}{2}} \tag{8}$$

Where S_{ij} is the stress deviator

$$S_{ij} = \sigma_{ij} - \frac{1}{3}\sigma_{kk}\delta_{ij} \tag{9}$$

The stress–strain relation is given by [4].

$$\begin{pmatrix} \sigma_{rr} \\ \sigma_{\varphi\varphi} \\ \sigma_{zz} \\ \sigma_{rz} \end{pmatrix} = \begin{pmatrix} c_{11} & c_{12} & c_{13} & 0 \\ c_{21} & c_{22} & c_{23} & 0 \\ c_{31} & c_{23} & c_{33} & 0 \\ 0 & 0 & 0 & c_{44} \end{pmatrix}\begin{pmatrix} \varepsilon_{rr} - \beta_{11}\Delta T \\ \varepsilon_{\varphi\varphi} - \beta_{22}\Delta T \\ \varepsilon_{zz} - \beta_{33}\Delta T \\ \varepsilon_{rz} \end{pmatrix} \tag{10}$$

From Distortional energy theory [4].

Distortion Strain Energy = Total Strain Energy − Volumetric strain Energy

$$\sigma_{\mathrm{vonMises}} = \frac{\sqrt{\left(\sigma_1 - \sigma_2\right)^2 + \left(\sigma_2 - \sigma_3\right)^2 + \left(\sigma_3 - \sigma_1\right)^2}}{2} \tag{11}$$

$$\sigma_{ex} = \begin{cases} 0, & \sigma_{von} \le \sigma_{\mathrm{crss}} \\ \sigma_{von} - \sigma_{\mathrm{crss}}, & \sigma_{von} > \sigma_{\mathrm{crss}} \end{cases} \tag{12}$$

σ_{ex} is the excessive stress, σ_{crss} is the critically resolved shear stress.

4 Result and Discussion

4.1 Temperature Distribution

The side and top heaters provide suitable control of temperature distribution in the DS system. The role of the side heater is to convey heat through thermal radiation for crucible support and then transfer it to the silicon feedstock in the crucible. The side heater has higher power than the top heater, which is used to maintain a convex melt-crystal interface shape during solidification. The heat is extracted through the heat exchanger block at the bottom via the process of slit valve opening. Due to the energy balance between input heat from the heaters and heat extraction at the bottom retort or heat exchanger block, the crystal begins to grow from the bottom of the crucible [20]. Temperature distribution plays a vital role in the crystal growth process, as it is one of the important factors determining the quality of the crystalline silicon ingot. Grain boundary, growth velocity, and interface shape can be controlled by temperature distribution. Figure 2 shows the temperature distribution of mc-Si ingots for both conventional and modified systems. After complete growth, the ingot from the modified system exhibits a lower temperature distribution compared to that from the conventional system. This is attributed to more heat being transferred in the carbon crucible due to its higher thermal conductivity compared to the quartz crucible.

4.2 Temperature Gradient

During the growth of multi-crystalline silicon, the temperature gradient can influence the quality of the ingot. Thermal

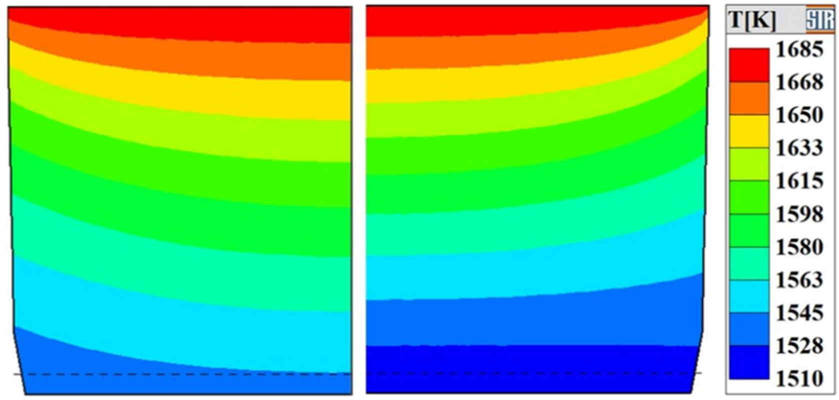

Fig. 2 Temperature distribution of mc-Si (left-conventional) and (right-modified)

stress and defects in the mc-Si ingot are related to the temperature gradient. A higher temperature gradient results in greater thermal stress, while a lower temperature gradient leads to less thermal stress. Figure 3 shows the temperature gradient of both conventional and modified systems. In this case, the temperature gradient was measured between the crystal and crucible at the bottom for both conventional and modified systems with different solidification fractions (25%, 50%, and 75%). The maximum temperature gradient occurs in the margin (centre) region, and the minimum temperature gradient occurs in the peripheral region for both conventional and modified systems. For all solidification fractions, the modified system has a lower temperature gradient compared to a conventional system. Normally, the thermal conductivity of carbon is higher than that of quartz at a particular temperature. The reduction in temperature gradient is due to the carbon materials of both the crucible and the heat exchanger block. This lower temperature gradient is more favorable for producing better-quality ingots.

4.3 Von Mises Stress

Thermal stress also affects the dislocation density and the quality of the multi-crystalline silicon ingot. Temperature distribution plays a vital role in thermal stress. If the temperature gradient is large, then the thermal stress will be high; hence, this should be controlled and kept at a minimum [21]. Thermal stress is caused by inhomogeneous temperature distribution or non-uniform thermal gradient. Von Mises stress is a type of thermal stress [22]. We can determine the von Mises stress using stress components from the distortion energy theorem [23]. The larger temperature gradient and inhomogeneity of temperature distribution are the main reasons for thermal stress in mc-Si ingot. Additionally, the thermal expansion of silicon, constrained by the crucible, may cause thermal stress. High critical thermal stress may cause the ingot to crack and release this stress. Figure 4 shows the von Mises stress of mc-Si ingot, revealing that the modified system has less von Mises stress compared to a conventional

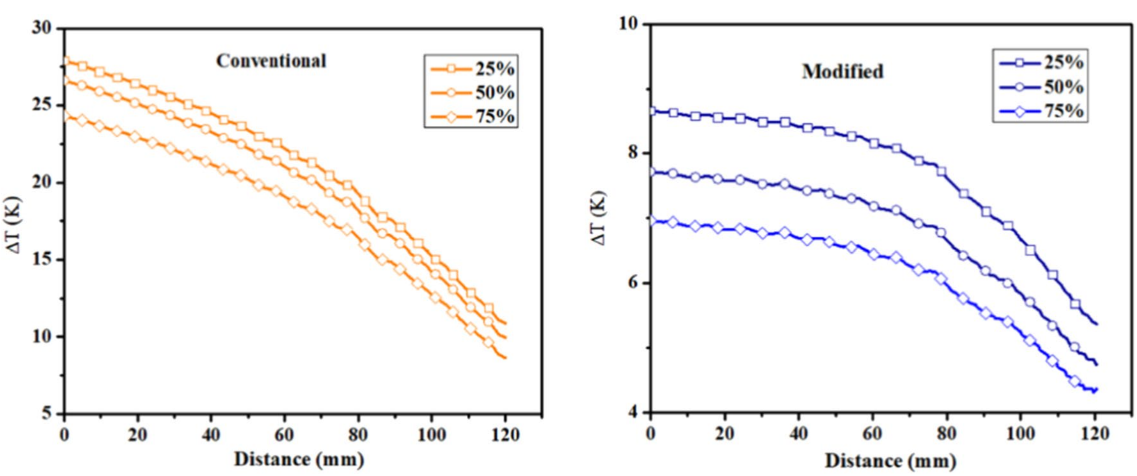

Fig. 3 Temperature gradient between crystal and crucible for different solidification

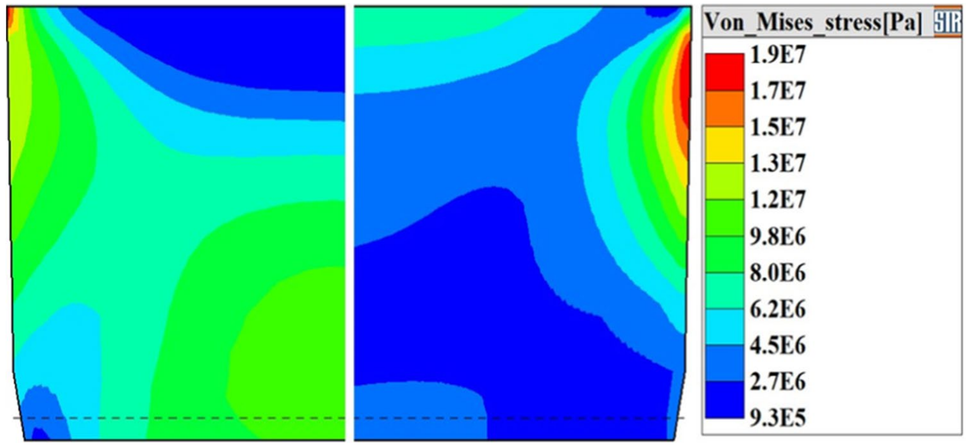

Fig. 4 Von Mises stress of mc-Si ingot (left-conventional) and (right-modified)

system. When comparing the thermal expansion coefficient of polysilicon with quartz and carbon, the difference in thermal expansion coefficient between polysilicon and carbon is less than that of quartz. This is why the modified system exhibits a better von Mises stress value than the conventional system.

4.4 Maximum Shear Stress

The maximum shear stress is generated by a heterogeneous temperature distribution. To better control shear stress, a more uniform temperature distribution is required during the DS process [23]. The presence of defects and dislocations is a major issue in the silicon crystal growth process. Dislocations are the primary restriction to increasing the efficiencies of solar cells in silicon ingots. Shear stress contributes to the generation of dislocations as well as defects in grown mc-Si ingots. Shear stresses involve the macroscopic shearing of material without changing the position of the unit cell. Due to temperature differences, shear stress occurs inside the ingot. Figure 5 reveals that the modified system has lower maximum shear stress compared to a conventional system. The maximum shear stress ranges from 5.1E5 to 9.8E6. From Fig. 5, in the modified system, the majority of regions of the grown ingot are covered in the range of 5.1E5 to 4.2E6, which was lower in conventionally grown ingots. The maximum shear stress ranges from 8.9E6 to 9.8E6 present in the ingots grown by a modified system. However, these ranges are covered in the red zone, which is not suitable for solar cell applications.

4.5 Normal Stresses

Once a force acts normal or perpendicular to an object's surface then it employs the normal stress. Normal stress acts in only one direction. Sigma 11, sigma 22, and sigma 33 are the types of normal stresses. By using the state of stress at a point, all the normal stress components combined to form the shear stress components that are the purpose for analyzing the normal stress.

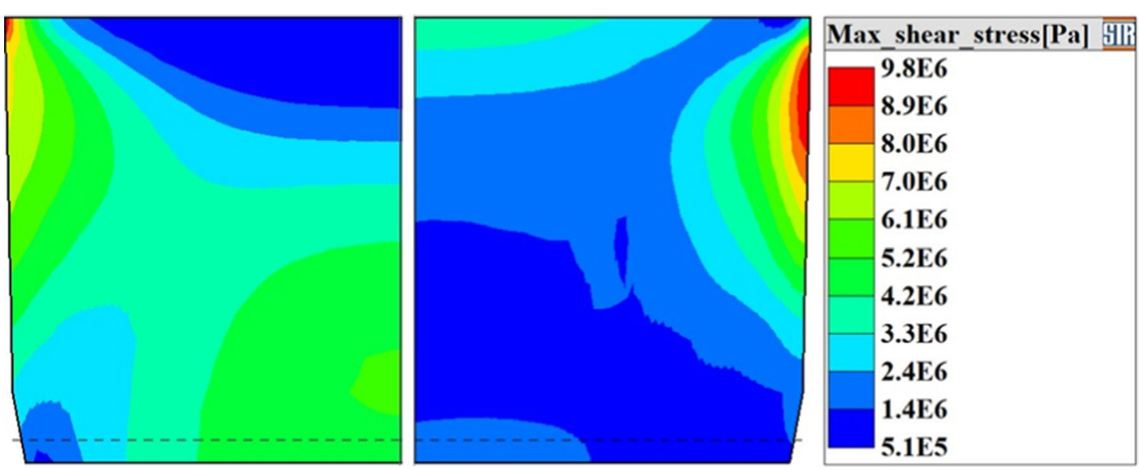

Fig. 5 Maximum Shear stress of mc-Si ingot (left-conventional) and (right-modified)

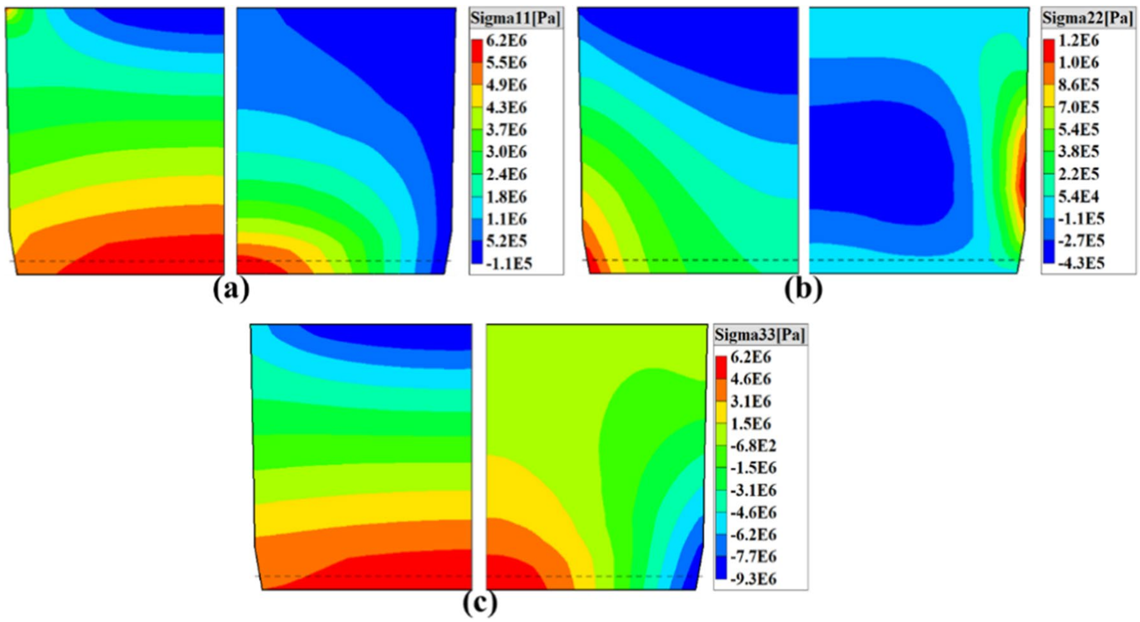

Fig. 6 Normal stress (sigma 11 (**a**), sigma 22 (**b**), sigma 33 (**c**)) of multi-crystalline ingots

4.5.1 Sigma 11, Sigma 22, Sigma 33

The Sigma 11 is a normal stress, this normal stress is the main cause of the defects in the mc-Si ingot. Figure 6a shows the normal stress sigma 11 of mc-Si ingot left side is conventional and the right side is modified. The modified system has less normal stress sigma 11. The sigma 22 is a normal stress, this normal stress is an important cause for stress distribution of homogeneous function [21]. Figure 6b shows the normal stress sigma 22 of mc-Si ingot, the left side is conventional, and the right side is modified. The modified system has less normal stress sigma 22. Especially the corner region of the ingot is not used for the solar cell application. For the modified system maximum sigma 22 is present at the corner region only. To get better quality mc-Si ingot the normal stress should be less with homogeneous distribution. Figure 6c shows the normal stress sigma 33 of mc-Si ingot left side is conventional and the right side is modified. The modified system has less sigma 33 normal stress and major regions are in the homogeneous distribution than the conventional system.

4.6 Power Consumption

The focus of photovoltaic industries is to grow superior-quality mc-Si ingots with low power consumption. Power consumption plays a leading role in the DS process because it can determine the price of the mc-Si silicon. Heat loss can also affect power consumption. The conventional system has a total power consumption of 203 kW, and the modified system has a total power consumption of 198 kW. While comparing both systems, the modified system saves up to 5 kW of power. Figure 7 reveals the total power consumption for both conventional and modified systems. The modified system has less power consumption than the conventional system. This is due to the material properties of the crucible. Carbon has larger thermal conductivity than quartz so there will be easy heat transmission in carbon crucible.

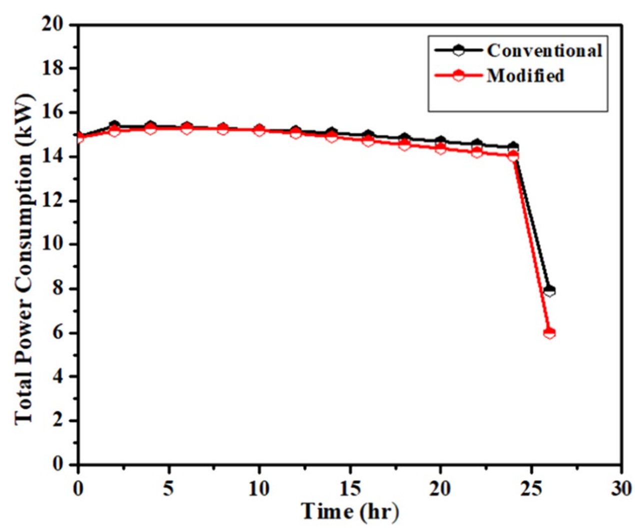

Fig. 7 Power Consumption of directional solidification process of multi-crystalline silicon ingot

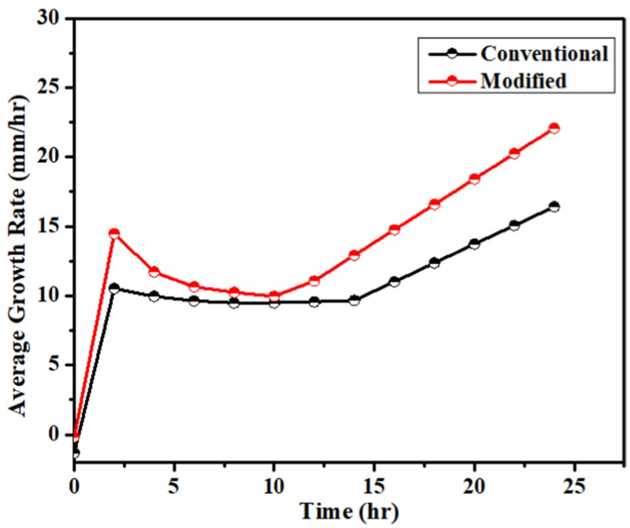

Fig. 8 Average growth rate of multi-crystalline silicon ingot during Directional Solidification process

4.7 Average Growth Rate

During the DS process growth rate can influence the quality of the mc-Si ingot. A slow growth rate can reduce the dislocation density and increase the quality. The manufacturing efficiency is increased by a fast growth rate but reduces the quality by initiating the defects. For industrial purposes, at the initial stage, there should be a slow growth rate, and at the final stage, there should be a fast growth rate to increase the manufacturing efficiency as well as crystal quality. Figure 8 reveals the average growth rate for both conventional and modified systems. From the initial stage, the modified system has a higher growth rate than the conventional system. From 2 to 10 h, the growth rate is slightly decreased from the initial stage for both conventional and modified systems, however, the modified system has a higher growth rate. After 10 h the growth rate increased linearly for both systems. The overall growth rate is higher for modified systems when compared with conventional systems. The average growth rate per hour for conventional and modified systems is 3.4 mm. and 4.4 mm. The average growth rate for the modified system has increased by 1 mm/hr when compared with the conventional system.

4.8 Carbon Distribution Analysis

The sources of carbon impurities in the growth system are graphite materials such as retort, heaters, and graphite shields. These three elements are common for both systems. In the modified system the additional graphite element of carbon crucible was used. Figure 9 shows the carbon concentration at the contact of the side crucible wall and the silicon melt for different solidification fractions (25%, and 50%). It reveals that the modified system has a higher carbon concentration than the conventional system. This is due to the presence of the carbon crucible.

Further, we have analyzed the carbon concentration in completely grown mc-Si ingot for both conventional and modified systems, and these results are shown in Fig. 10. The segregation coefficient of carbon with silicon melt is 0.07, hence the carbon atoms move towards the melt-free surface and the segregated at the top region of the ingot. The carbon transport mechanism can be described by the fundamental reaction that happens when graphite and silicon contact at high temperatures. Carbon from the

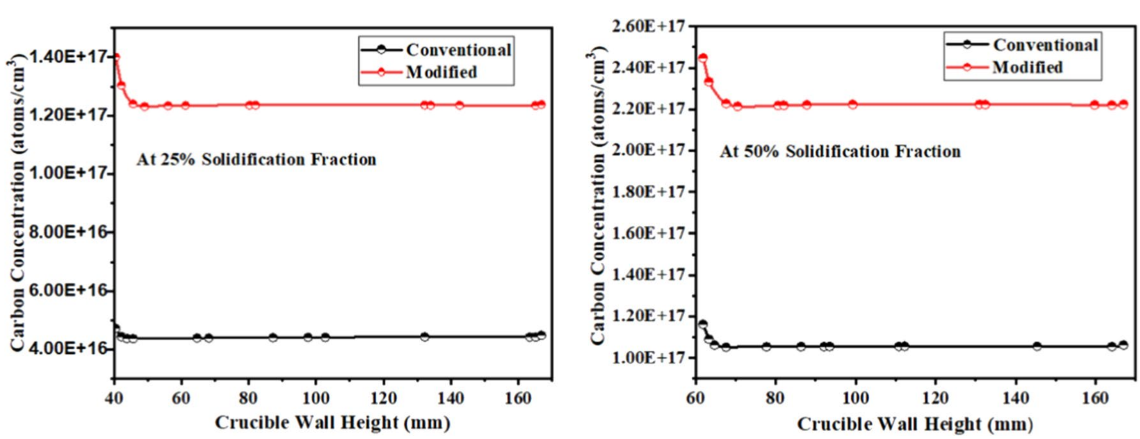

Fig. 9 Carbon concentration at the interface of crucible wall and silicon melt

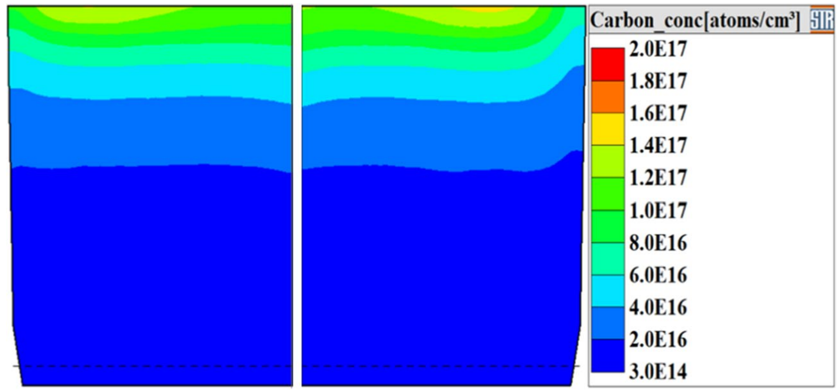

Fig. 10 Carbon concentration in mc-Si ingot (left-quartz crucible) and (right-carbon crucible)

crucible wall and silicon dioxide from raw silicon material react together, and the following equation is described by

$$SiO_2(solid) + 2C(solid) \rightarrow Si(solid) + 2CO(gas)$$

The carbon concentration is slightly higher for the carbon crucible mc-Si than the quartz crucible mc-Si that is present in the red zone. This is due to the presence of a carbon crucible in the DS system. The quartz and the carbon crucible are coated with silicon nitrate with the same thickness (25 microns). This coating is more useful for reducing the carbon concentration in the mc-Si ingot during the growth process.

5 Conclusion

The silicon nitride-coated carbon crucible DS furnace has been simulated by crystal growth simulation software. This numerical simulation is based on the finite volume method. The effect of silicon nitride-coated carbon crucible in the mc-Si ingot has been analyzed and results were compared with the silicon nitride-coated quartz crucible. The input parameters of argon flow, heater temperature, and slit valve opening are common for both systems. The quality of mc-Si ingots and power consumption have been compared. Further, the temperature gradient, von mises stress, maximum shear stress, and normal stresses (sigma 11, sigma 22, and sigma 33) have been simulated and results were compared. The modified system has less temperature gradient, which is suitable for growing good-quality mc-Si ingot. Further, the von Mises stress, maximum shear stress, and normal stresses are less in the modified system. Silicon nitride-coated carbon crucible takes less power consumption and a slightly higher average growth rate when compared with silicon nitride-coated quartz crucible, which is more suitable for industrial purposes. Finally, we have analyzed the carbon distribution in mc-Si grown by both systems. The mc-Si ingot grown by carbon crucible has a slightly higher carbon concentration in the red zone only. The whole ingot is useful for solar cell applications except for the outer red zone region. Therefore, the silicon nitride-coated carbon crucible DS system is more favourable for producing better quality mc-Si with less production cost.

Acknowledgements This work is supported by the Department of Science and Technology, Government of India (Order No. DST/TMD/CERI/RES/2020/7 dated 31/12/2020).

Author Contributions All authors contributed to the study's conception and design. Material preparation, data collection, and analysis were performed by 1.P. Periyannan, 2. M. Bharathwaj, 3. Dr. P. Karuppasamy, and 4. Dr. P. Ramasamy. The first draft of the manuscript was written by P. Periyannan. All authors read and approved the final manuscript.

Funding This work was supported by the Department of Science and Technology (DST), Government of India (Order. no: DST/TMD/CERI/RES/2020/7, dated 31/12/2020).

Data Availability No datasets were generated or analysed during the current study.

Declarations

Ethics Approval We comply with ethical standards. We provide our consent to take part.

Consent to Participate and Publication The authors consent to participate and publication.

Competing Interests The authors declare no competing interests.

References

1. Kerkar F, Kheloufi A, Dokhan N, Ouadjaout D, Belhousse S, Medjahed S, ... Laib K (2020) Oxygen and carbon distribution in 80Kg multicrystalline silicon ingot. Silicon 12:473–478

2. Muthukumar R, Aravinth K, Bhargav PB, Ramasamy P (2023) Numerical investigation on effect of side heater modification on the stress distribution and dislocation density of multi-crystalline silicon ingot grown by DS process. Silicon 15(18):7755–7764
3. Anbu G, Srinivasan M, Ramasamy P (2019) Modeling on modified heater design of DS system for improving the quality of mc-silicon ingot. Silicon 11:1393–1400
4. Keerthivasan T, Aravindan G, Srinivasan M, Ramaswamy P (2022) Effect of partial replacement of retort with an insulation material on mc-silicon grown in directional solidification furnace: Numerical Modeling. Silicon. pp 1–8
5. Nagarajan SG, Sanmugavel S, Kesavan V, Aravindan G, Srinivasan M, Ramasamy P (2019) Influence of additional insulation block on multi-crystalline silicon ingot growth process for PV applications. J Cryst Growth 516:10–16
6. Ma W, Zhong G, Sun L, Yu Q, Huang X, Liu L (2012) Influence of an insulation partition on a seeded directional solidification process for quasi-single crystalline silicon ingot for high-efficiency solar cells. Sol Energy Mater Sol Cells 100:231–238
7. Zhang H, Zheng L, Ma X, Zhao B, Wang C, Xu F (2011) Nucleation and bulk growth control for high efficiency silicon ingot casting. J Cryst Growth 318(1):283–287
8. Wu Z, Zhong G, Zhang Z, Zhou X, Wang Z, Huang X (2015) Optimization of the high-performance multi-crystalline silicon solidification process by insulation partition design using transient global simulations. J Cryst Growth 426:110–116
9. Ding C, Huang M, Zhong G, Ming L, Huang X (2014) A design of crucible susceptor for the seeds preservation during a seeded directional solidification process. J Cryst Growth 387:73–80
10. Anbu G, Nagarajan SG, Aravindan G, Srinivasan M, Ramasamy P (2021) Influence of additional insulation block on melt-crystal interface shape in directional solidification system for growing high quality mc-silicon ingot: a simulation investigation. Silicon 13:1713–1722
11. Zhang Z, Yu X, Yang D (2022) A New Design of Side Heater for 3D Solid-liquid Interface Improvement in G8 Directional Solidification Silicon Ingot Growth. Silicon 14(15):9407–9416
12. Kesavan V, Srinivasan M, Ramasamy P (2019) The influence of multiple-heaters on the reduction of impurities in mc-Si for directional solidification. Silicon 11:1335–1344
13. Wei J, Zhang H, Zheng L, Wang C, Zhao B (2009) Modeling and improvement of silicon ingot directional solidification for industrial production systems. Sol Energy Mater Sol Cells 93(9):1531–1539
14. Nguyen THT, Chen JC, Hu C, Chen CH, Huang YH, Lin HW, ... Hsu B (2017) Numerical analysis of thermal stress and dislocation density distributions in large size multi-crystalline silicon ingots during the seeded growth process. J Cryst Growth 468:316–320
15. Bharathwaj M, Sugunraj S, Karuppasamy P, Srinivasan M, Ramasamy P (2023) Effect of argon flow rate on mc-silicon ingot grown by DS process for PV application: a numerical investigation of non-metallic impurities. Silicon 15(14):5937–5946
16. Smirnova OV, Mamedov VM, Kalaev VV (2014) Numerical modeling of stress and dislocations in Si ingots grown by seed-directional solidification and comparison to experimental data. Cryst Growth Des 14(11):5532–5536
17. Sekar S, Gurusamy A, Manikkam S, Perumalsamy R (2023) Improvement of DS grown Mc-Si Ingot for PV application by reducing the thickness of the bottom heat exchanger block: numerical investigation. Silicon 15(10):4183–4192
18. Alexander H, Haasen P (1969) Dislocations and plastic flow in the diamond structure. In Solid state physics, vol 22. pp 27–158 (Academic Press)
19. Chen XJ, Nakano S, Liu LJ, Kakimoto K (2008) Study on thermal stress in a silicon ingot during a unidirectional solidification process. J Cryst Growth 310(19):4330–4335
20. Kumar MA, Aravindan G, Srinivasan M, Ramasamy P, Kakimoto K (2022) Numerical analysis of melt flow and interface deflection during the growth of directional solidified multi-crystalline silicon ingots of three different dimension. Silicon. pp 1–9
21. Gurusamy A, Thiyagarajan M, Srinivasan M, Ramasamy P (2023) Numerical investigation on modified bottom heater of DS furnace to improve mc-Si ingot. Silicon 15(8):3713–3724
22. Song B, Luo Y, Rao S, Zhang F, Hu Y (2020) Numerical simulation on Design of Temperature Control for side heater in directional solidification system of multi-crystalline silicon. Silicon 12(9):2179–2187
23. Gopalakrishnan A, Madhu T, Gurusamy A, Manickam S, Perumalsamy R (2023) Investigation of DS Furnace Heat Exchange Block Thickness for the Improvement mc-Si Ingot Quality. Silicon 15(5):2185–2197